Optimization of Cyclopropylamine Plasma Polymerization toward Enhanced Layer Stability in Contact with Water

Anton Manakhov, Lenka Zajíčková,* Marek Eliáš, Jan Čechal, Josef Polčák, Jaroslav Hnilica, Štěpánka Bittnerová, David Nečas

The present investigation of cyclopropylamine (CPA) plasma polymerization in pulsed and continuous wave radio frequency (RF) discharges leads to the proposition of conditions at which amine-rich films exhibit a good stability in contact with water. The analyses reveal complex structure of CPA plasma polymers containing hydrocarbon chains, primary and secondary amines, nitriles and possibly imines. The decomposition of the monomer in plasma is progressing with the composite parameter *W/F* (RF power over monomer flow rate) but, in pulsed discharges, it is possible to deposit the films with N/C ratio above 0.24 using higher monomer flow rate. At the optimized monomer flow rate the 280 nm thick film exhibits only 20% thickness loss after 48 h immersion in water and still contains about 5 at% of the $\underline{N}H_x$ environment.

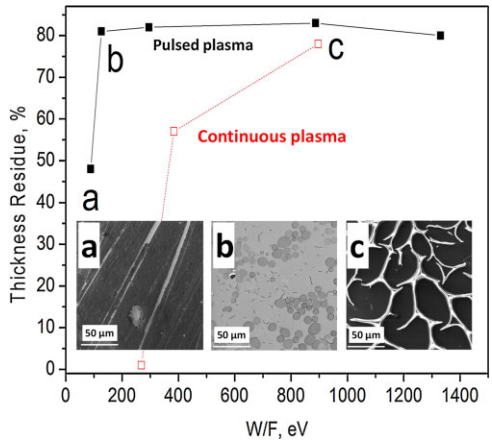

1. Introduction

The deposition of stable amine-rich thin films has attracted attention of numerous researchers due to its great potential applications, such as biomolecule immobilization,[1] micro-filtration membranes,[2] enzyme electrodes,[3] adhesion enhancement,[4] or biosensor development.[5] The simplest technique of amine grafting relies on plasma treatment in nitrogen or ammonia discharges.[6] However, these techniques lead to unstable functionalization of a thin near surface layer with rather short duration. It has been observed that the grafted groups almost disappeared after several days of ageing in air, and the composition of the surface became comparable with the untreated layer.[7] In contrary, the deposition of plasma polymers can enhance the stability of the surface and reduce the aging effect.[1] For many years, allylamine has been the monomer of choice thanks to the presence of vinyl groups that enable free radical polymerization of this amine compound. However, allylamine is a highly toxic flammable chemical compound with a lethal dose LD_{50} equal to 35 mg kg^{-1}.[8] Moreover, the amine-rich plasma polymerized allylamine thin films showed a significant decrease in nitrogen concentration (N/C decreasing from 0.22 to 0.06)[9,10] and film thickness loss up to 90% after the immersion in water.[11] The stability can be improved by an increase of plasma power at the expense of amine concentration in the films.[12]

The application of amine-rich thin films for cell adhesion enhancement or biosensing requires high stability of the layer in aqueous media and prevention of trapped toxic molecules. Therefore, substituents of the allylamine

Dr. A. Manakhov, Prof. L. Zajíčková, Dr. M. Eliáš, Š Bittnerová, Dr. D. Nečas
Plasma Technologies, CEITEC – Central European Institute of Technology, Masaryk University, Kotlářská, 2, Brno 61137, Czech Republic
E-mail: lenkaz@physics.muni.cz
Dr. J. Čechal, Dr. J. Polčák
CEITEC – Central European Institute of Technology, Brno University of Technology, Technická 3058/10 616 00 Brno, Czech Republic
Dr. J. Hnilica
Faculty of Science, Department of Physical Electronics, Masaryk University, Kotlářská 2, Brno 61137, Czech Republic

monomer are highly required. Recently, it was found that copolymerization of acetylene and ammonia or ammonia and ethylene leads to the deposition of stable amine coatings (thickness loss ≈15%) bearing around 5 at% of amine groups, if a high flow rate of C_2H_4 or C_2H_2 is used.[6,13] Nevertheless, in order to obtain even higher concentration of the amine groups, a high flow rate of ammonia is necessary and the coatings deposited in these conditions suffer from thickness loss (up to 70%) after an immersion in water. By plasma polymerization of *n*-heptylamine it is possible to deposit sufficiently stable (thickness loss ≈15%) amine coatings but the concentration of amine groups and nitrogen in such films is significantly lower compared to the allylamine plasma polymers (N/C ∼ 0.12).[14] Another promising technique for the amine-rich coating deposition is the plasma polymerization of the isomer of allylamine, cyclopropylamine (CPA). As reported, a low pressure inductively coupled plasma (ICP) polymerization of CPA led to a higher amine deposition efficiency compared to allylamine plasma polymerized layers.[15] Although CPA is non-toxic and has a high vapor pressure of 32 kPa at 25 °C, the investigation of CPA plasma polymerization has been quite limited and no tests regarding the CPA plasma layer stability are available.

Beside the problems with the stability of amine films in water, a degradation of surface amine groups occurs during storage, i.e., during the period between the preparation and use of the layers. According to the literature, whatever the method of amine coating deposition is applied, the amine layers are degrading rapidly in air.[1] However, it was found that the storage of plasma polymerized amine films in nitrogen atmosphere at −20 °C almost prevents their degradation.[16]

In this work, the low pressure capacitively coupled plasma (CCP) polymerization of CPA was studied for wide range of energies (*W*/*F*) and stability of the resulting plasma polymers after the immersion in water. According to the literature, the composite parameter *W*/*F*, calculated as the radio frequency (RF) power over the monomer flux, strongly influences the properties of plasma polymers including their chemical composition and stability.[17–19] The broad range of *W*/*F* in the present study was achieved by varying the monomer flow rate and pulsing the RF discharge. The properties of the pulsed wave (PW) and continuous wave (CW) plasma polymers are compared because pulsing can strongly affect the monomer degradation[20,21] or decrease the compressive stress.[22]

2. Experimental Section

2.1. Materials

Cyclopropylamine (Figure 1) with a purity of 98% was purchased from Sigma–Aldrich and used as the monomer for plasma polymerization without any further purification. Argon in the purity of 99.998% was supplied by Messer. Double-side polished silicon single crystal ⟨111⟩ (N-type phosphorus doped) substrates with the resistance 0.5 Ω cm were used for the deposition. All substrates were cleaned by sonication in the isopropanol (Penta, 99.8%) for 10 min.

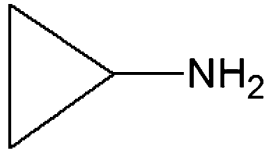

Figure 1. Chemical sketch of CPA.

2.2. Plasma Polymerization Set-Up

The CPA plasma polymers were deposited onto silicon substrates by using low pressure CCP discharges operating at the frequency of 13.56 MHz. The CCP reactor was a horizontally mounted glass tube, 8 cm in diameter, closed by two aluminum electrodes (Figure 2). The perforated grounded electrode enabled gas feeding whereas the perforated RF electrode was used to pump the reactor by a rotary pump. The distance between the grounded and RF electrodes was 18.5 cm. The silicon substrates were placed on the glass holder 5 cm from the RF electrode in the height of 4 cm from the bottom of the glass tube. Therefore, the substrate potential was equal to the floating potential estimated according to literature[23] as maximum 15 V in this type of discharge.

Prior to the deposition, the substrates were cleaned for 10 min by squared pulsed Ar plasma at on-time power of 20 W and pressure 120 Pa. Different plasma conditions of the deposition, summarized in Table 1, were tested at the total pressure of 120 Pa. The flow rate of Ar was set to 28 sccm and regulated by electronic flow controller Hastings, whereas the flow rate of CPA vapors was set by a needle valve. For all pulsed plasma conditions, the pulse repetition function (PRF) and duty cycle (DC) were set to 500 Hz and 33%, respectively. Hence, the corresponding plasma time-ON (T_{ON}) and time-OFF (T_{OFF}) were kept equal to 660 and 1 340 μs, respectively.

The composite parameter *W*/*F* and the mean power W_{mean} were calculated according to Equation (1) and (2), where *W* is power delivered by the RF generator (Watt), *F* is the flux of monomer given in standard liters per second, V_m is the molar volume of the gas

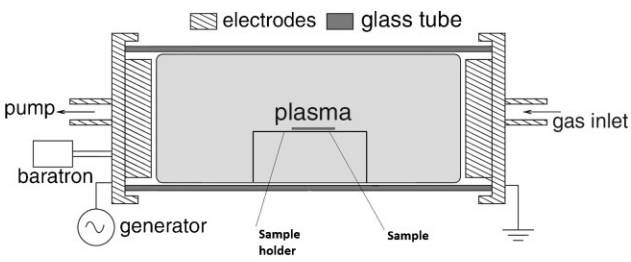

Figure 2. Plasma polymerization set-up.

DOI: 10.1002/ppap.201300177

Table 1. Summary of plasma conditions used for the CPA plasma polymerization.

Monomer flow rate [sccm]	DC [%]	On-time power [W]	W_{mean} [W]	W/F [eV]	Deposition rate [nm s^{-1}]
1	33	20	6.6	88.7	0.2
1	100	20	20	268.8	0.5
0.7	33	20	6.6	126.7	0.3
0.7	100	20	20	384.0	0.3
0.3	33	20	6.6	295.7	0.3
0.3	100	20	20	896.1	0.2
0.1	33	20	6.6	887.1	0.1
0.1	33	30	9.9	1330.6	0.1

(L mol^{-1}), N_A is Avogadro constant and 1.602×10^{-19} is a modulus of the electron charge.

$$W_{mean} = W \times \frac{T_{ON}}{T_{ON} + T_{OFF}} \quad (1)$$

$$W/F = \frac{W_{mean}}{F/V_m} \times \frac{1}{N_A} \times \frac{1}{1.602 \times 10^{-19}} \quad (2)$$

Then, the values of W/F are expressed in eV similarly as described elsewhere.[17] The W/F value does not represent correctly the energy invested per monomer molecule because it is not corrected for power losses outside plasma, the energy absorbed by Ar atoms[24] and plasma expansion. However, W/F allows relative comparison of energetic conditions for changed monomer flow rate and mean RF power because power losses and plasma expansion were similar in all the conditions used.

The deposition time was adjusted in order to obtain the film thickness of 280 ± 30 nm except the layers deposited at the monomer flow rate of 0.1 sccm due to the extremely low deposition rate at this particular condition. The thickness of these samples was about of 120 nm.

2.3. Optical Emission Spectroscopy

Optical emission spectroscopy (OES) has been carried out using a Jobin Yvon Horiba FHR1000 spectrometer (Czerny-Turner configuration) with ≈1 m focal length and ≈2 400 grooves mm^{-1} grating. An intensified CCD camera (Andor IStar 720) at the exit port of the spectrometer served as the detector. The specified spectral resolution is ≈8 pm and the time resolution is in order of nanoseconds. The relative spectral sensitivity of the spectrometer was calibrated using a tungsten-halogen lamp in spectral range from ≈200 to 750 nm.

The optical fiber was placed 10 mm from the discharge tube, perpendicularly to the discharge axis and it collected light above the sample holder. The overview spectra were recorded with integration time adjusted to achieve good data quality in the areas of Ar I lines (696–739 nm) and in the CN band ($B^2\Sigma^+ \rightarrow X^2\Sigma^+$, 382–388 nm).

2.4. XPS

For the characterization of plasma polymer layers, the Omicron X-ray source (DAR400) and electron spectrometer (EA125) fitted on custom built UHV system were used at pass energy of 25 eV and power of 270 W. The analysis area was circular with diameter approximately 1 mm and the electrons take off angle was set to 50°. All measurements reported in this paper were performed directly at a sample surface without any etching, additional treatment or manipulation. The quantification was carried out using XPS MultiQuant software.[25]

The XPS C1s, O1s and N1s signals were fitted by the CasaXPS software after subtraction of the Shirley-type background. The XPS data curve fittings were performed in accordance with the available literature on binding energies of different carbon and nitrogen environments.[26,27] The fitting employed Gaussian–Lorentzian (G–L) peaks with the fixed G–L percentage 30%. The full width at half maximum (FWHM) was set to 1.8 ± 0.05 eV for all the peaks.

2.5. Optical Characterization (FT-IR and Ellipsometry)

The ellipsometric data were measured in the spectral region of 0.6–6.5 eV using a phase modulated Jobin Yvon UVISEL ellipsometer at angle of incidence equal to 65°. The optical data obtained for as-deposited films on Si and dried films on Si after immersion in water were fitted by the model of one homogeneous non-uniform film on Si substrate using a PJDOS dispersion model for SiO_2-like materials,[28] assuming a wedge-shaped non-uniformity.[29] The following parameters were fitted: thickness, thickness non-uniformity, and dispersion model parameters describing the electronic structure.

The very good agreement between the data and the fit achieved for all the as-deposited films revealed that the assumption of the homogeneous film in the direction perpendicular to the substrate was valid. After immersion in water, the films exhibited defects like surface roughness or inhomogeneity but the determination of the film thickness using the above mentioned structural model was still possible with a sufficient precision.

Fourier-transformed IR (FT-IR) spectra were obtained in the transmission mode using a Bruker Vertex 80v spectrophotometer

with accessory for a correct transmittance measurement in the spectral range from 370 to 7 500 cm^{-1}. The data were collected at pressure of 2.5 mbar with the resolution of 4 cm^{-1} and 500 scans. The transmittance of the films on Si substrate was divided by the transmittance of bare Si substrate and the resulting relative transmittance was used to calculate the film absorbance[30] that was subsequently normalized to the film thickness. In this paper, the FT-IR spectra are shown only in the range from 1 490 to 3 650 cm^{-1} because no significant absorption peaks belonging to the films were identified outside this range and the identification of weak absorption peaks below 1 490 cm^{-1} was difficult due to the strong absorption peaks in Si that could not be reliably subtracted.

2.6. SEM

The plasma polymer surface images were analyzed using the field-emission scanning electron microscope (FE-SEM) LYRA3 XM, manufactured by Tescan. The instrument provided an extremely high contrast during the complex morphology investigation. In all measurements, the electrons were accelerated by a 2 kV high voltage and the working distance was fixed at ≈5 mm in order to minimize the charging effect. Images with resolution of 1 024 × 1 144 pixels were acquired within ≈1 minute. The SEM analyses were performed directly at the sample surface without any conductive coating deposition.

2.7. Stress Measurement

The radii of curvature of the coated and non-coated Si substrates were measured three times using a Brucker DektakXT-A surface profilometer. The residual compressive stress of the films was calculated using Stoney's equation, as described elsewhere.[31]

2.8. Tests of Stability of Layers in Water

In order to evaluate the stability of plasma polymers in aqueous media, the deposited layers were immersed in a deionized water (volume of ≈5 mL) for 1, 24, and 48 h. Immediately after the immersion, ellipsometry and FT-IR analyses were performed, while XPS and SEM analyses were carried out 2 d after immersion test.

3. Results and Discussion

3.1. Influence of Discharge Parameters on Chemistry of CPA Plasma Polymers

As CPA plasma polymerization has not yet been thoroughly studied, all important parameters, such as plasma power, DC, and monomer flow rate had to be optimized for the deposition of stable amine-rich layers. Tuning all these parameters separately may require the testing of a huge number of samples. As discussed in the Section 1, it is generally assumed that low pressure plasma polymerization can be essentially controlled by W/F. Changes of RF power led in our experimental configuration to significant changes of the discharge character. Therefore, the variation of W/F in the range from 88 to 1 330 eV was achieved by varying the monomer flow rate and DC. Since thinking of DC as the parameter influencing the power delivered into the discharge can cause an oversimplification of the deposition process, the properties of plasma polymers prepared in both, CW and PW, modes at a similar W/F were compared.

In general, the polymerization of CPA in CCP led to the deposition of homogenous and adherent layers. According to SEM micrographs, the films were smooth and free of cracks or pinholes. FT-IR analyses revealed that whatever conditions were used the CPA plasma polymers contained CH_x, NH_x, and C≡N groups (Figure 3). The assignment of the IR absorption peaks, reported in Table 2, was performed on the basis of comprehensive IR data.[32,33] The presence of primary amine groups was confirmed by the presence of NH_2 asymmetric and symmetric stretches accompanied with the NH_2 scissoring band at 3 430, 3 365, and 1 640 cm^{-1}, respectively. The peak at 1 640 cm^{-1} can also contain a small contribution of imine function C═N. Additionally, the presence of amide groups cannot be completely excluded due to the overlap of amide II band (C═O stretching) and NH_2 scissoring. However, the characteristic NH bending of amide group at ≈1 550–1 600 cm^{-1} was not clearly visible and XPS analyses showed a relatively low content of oxygen (Table 3). Secondary amines could be also present in the films because the position of >N—H stretching overlaps with —NH_2 symmetric stretching. The structure of the CH_x stretching

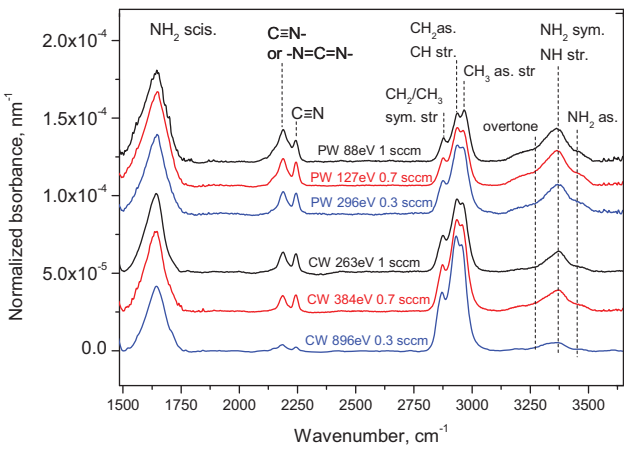

Figure 3. Normalized absorbance of CPA plasma polymers deposited at fixed power of 20 W in pulsed and continuous wave modes (PW and CW, respectively) at three different monomer flow rates, 1.0, 0.7, and 0.3 sccm. The type of the mode, the W/F and the monomer flow rate are given in the figure for each spectra. The normalized absorbances are shifted in order to separate the curves.

DOI: 10.1002/ppap.201300177

Table 2. Identification of the absorption peaks in IR spectra.

Type of vibration	Wave number [cm^{-1}]	Type of vibration	Wave number [cm^{-1}]
NH_2 asym. str.	3 430	C—H_2 asym. and C—H str.	2 930
NH_2 sym. and NH str.	3 365	CH_3 asym. str.	2 965
NH_2 sciss. overtone	3 265	CH_3 and C—H_2 sym. str.	2 870
C≡N str.	2 245	C≡N— and —N═C═N— str.	2 190
—NH_2 sciss.	1 640	C═O str.	1 690
NH bend. (amide)	1 550–16 00	C═N— str.	1 640–1 690

band observed below 3 000 cm^{-1} is complex because this band consists of CH_3, CH_2, and possibly CH (tertiary sp^3 carbon) stretching. The nitrile (C≡N), isonitrile (C≡N—) and/or conjugated imines (—N═C═N—) were identified in the FT-IR spectra as a double peak at 2 245 and 2 190 cm^{-1}.

It can be seen from Figure 3 that the intensities of the peaks attributed to the monomer structures (NH_2 stretching and NH_2 scissoring) are significantly higher for pulsed plasmas compared to the CW deposition at the same on-time power. It evidences that PW conditions lead to higher retention of the monomer structure. Therefore, the concept of W_{mean} as the parameter governing plasma chemical processes could be applied for the comparison of CW and PW conditions. Interestingly, the nitrile (C≡N) and isonitrile (C≡N—) bands were present in the spectra of all plasma polymers although CPA contains neither C≡N nor C≡N— functionalities.

The FT-IR analyses revealed that the structure of the CH_x stretching band depends on the monomer flow rate. As shown in Figure 3, the films deposited at 1 sccm of CPA in both, CW and PW, modes exhibited slightly higher intensity of CH_3 than CH_2/CH asymmetric stretching peaks, while it is reversed at 0.7 sccm or lower flow rates. It suggests a higher cross-linking of the films deposited at lower monomer flow rates, as these layers contain more "polymer-propagating" —CH_2— or >CH— groups compared to the "polymer-terminating" —CH_3.

In order to compare changes of the deposition conditions associated with either pulsing or change of the monomer flow, the W/F defined by Equation (2) is further used as the macroscopic parameter describing the influence of the plasma conditions on the polymer structure. The ratio I_{CN}/I_{CH}, the area integrated from 2 300 to 2 055 cm^{-1} divided by the band area from 3 050 to 2 800 cm^{-1}, is shown in dependence on W/F in Figure 4. It can be seen that the content of CH_x is increasing at the expense of CN for increased W/F. Therefore, the decomposition of the monomer into CN groups cannot be explained by a higher energy input and it is discussed below on the basis of XPS results and OES of the discharge.

The content of NH_2 groups is the fingerprint of monomer retention. Unfortunately, the stretching of NH_2 could not be

Table 3. The elemental composition of the CPA plasma polymers as deposited (before immersion in water) and after immersion in H_2O.

Disch. mode, *W/F* [eV]	C [at%]		N [at%]		O [at%]		Si [at%]	
	Before	After	Before	After	Before	After	Before	After
	Immersion in water		Immersion in water		Immersion in water		Immersion in water	
PW 88	78	78	20	16	2	6		
PW 127	78	77	19	15	3	8		
PW 296	78	77	17	14	5	9		
PW 887	78	77	16	14	6	9		
CW 268	79	63	16	12	5	15	0	10
CW 384	80	79	15	13	5	8		
CW 896	83	82	11	7	6	11		

The duration of the immersion is equal to 48 h for PW plasma layers while CW layers were immersed for 1 h.

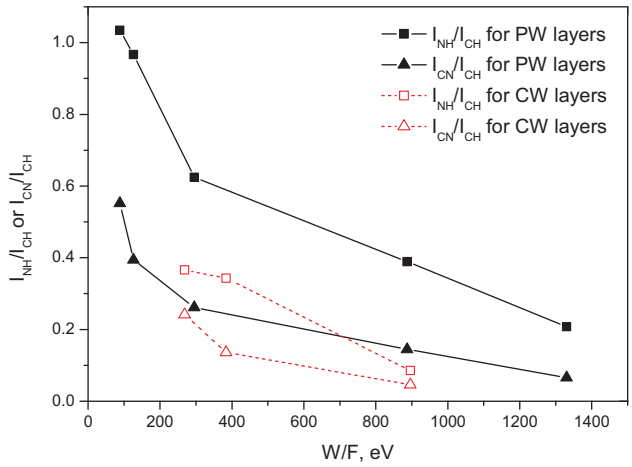

Figure 4. The ratio of the areas under NH and NH_2 stretching peaks (I_{NH}) and under CN stretching peak (I_{CN}) normalized to the area of CH_x stretching peak (I_{CH}) as a function of *W/F*.

clearly separated from NH and, therefore, the whole stretching band from 3 530 to 3 130 cm^{-1} was integrated in order to obtain I_{NH}. The ratio I_{NH}/I_{CH} is shown in dependence on *W/F* in Figure 4. The obtained tendency suggests higher monomer degradation with increased *W/F* and reveals that PW and CW depositions with the same *W/F* are not comparable in the final plasma polymerization product.

In order to confirm the FT-IR results, the samples were analyzed by XPS. The analyses revealed that the films also contain oxygen in the amount from 2 to 6 at% (Table 3). The presence of oxygen was not detected undoubtedly by FT-IR because the absorption of OH stretching falls into the same region as NH_2 band. The presence of oxygen is most probably related to the oxygen uptake after exposure of the amine layer to air, as it was reported before.[15] According to the literature,[1,34] the plasma polymers contain a substantial amount of free radicals that are trapped in the layer during plasma polymerization. The subsequent reactions of these radicals with oxygen during the exposure to air induce the incorporation of the oxygen-containing functionalities. The increase of the oxygen concentration with *W/F* should be related to the higher amount of trapped free radicals in the amine layers deposited at higher energy input.

The in-depth homogeneity of the films was tested by the preparation of a set of films with four different thicknesses (30, 120, 210, and 300 nm) deposited in PW mode at $W/F = 127$ eV using different deposition times. The C, N, and O concentrations were equal to 78.4 ± 0.3, 19.6 ± 0.3, and 2.1 ± 0.3 at%, respectively, for all four films, i.e., the variation of the film composition was within the range of the experimental errors.

The N/C ratio decreased with *W/F* as shown in Figure 5. It confirmed the FT-IR results that the monomer structure is less retained for higher energy input and that the same *W/F* does not produce similar plasma polymers in CW and PW modes. The decrease of the N/C ratio is slower for the PW mode and it is comparable to unpolymerized monomer at low *W/F*. Nevertheless, even approximation of the curve to *W/F* equal to 0 cannot produce N/C of 0.33 as in pure monomer. Indeed, CPA does not undergo classical free radical polymerization and therefore the propagation of the polymerization process is not possible without substantial addition of free radicals by the decomposition of the monomer. However, the pulsing of the discharge seems to be a very efficient method to suppress the degradation of the monomer structure.

The XPS C1s, N1s, and O1s curve fittings revealed the details with regard to the carbon and nitrogen environments evolution with *W/F*. A typical fitting of XPS C1s, N1s, and O1s signals obtained on CPA plasma polymer is depicted in Figure 6. In accordance with the FT-IR results, the N1s signal of all the films was fitted with a sum of three components corresponding to the main nitrogen environments, amine group (**N**$H_{x=1,2}$ ~ 399.0 eV), nitrile group (**N**≡C ~ 399.7 eV) and amide group (**N**—C═O ~ 400.3 eV). The C1s signal was fitted with a sum of four components corresponding to hydrocarbons (**C**H_x ~ 285.0 eV, used for binding energy calibration), carbon bonded to amine group (**C**—NH_x ~ 285.9 eV), carbon of nitrile group and carbon singly bonded to nitrile group (—**C**≡N/**C**—C≡N ~ 286.5 eV), and carbon double bonded to oxygen (N—**C**═O/—**C**═O ~ 288.0 eV). The oxygen spectra were fitted with two components, namely: acetal and ketone groups (**O**—C—**O**/—C═**O** ~ 532.7 eV) and amide group (**O**═C—N ~ 531.2 eV).

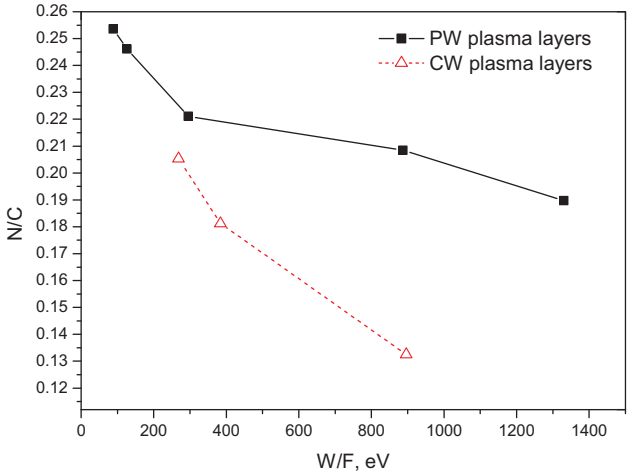

Figure 5. Evolution of N/C ratio as a function of *W/F* estimated by XPS.

DOI: 10.1002/ppap.201300177

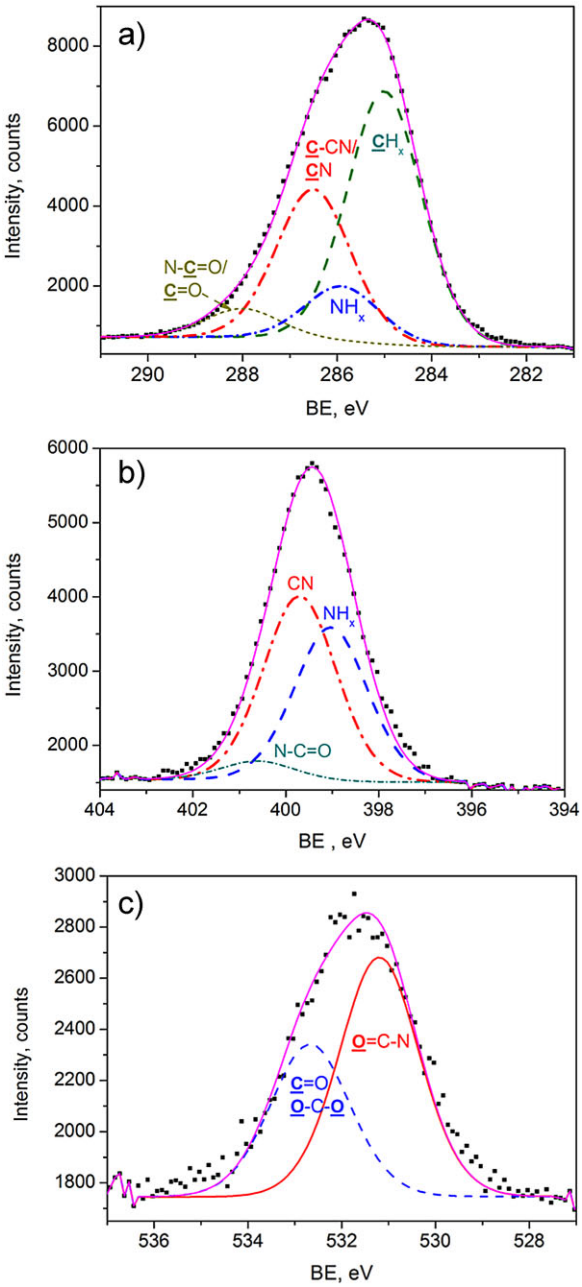

Figure 6. Fitting of XPS peaks of CPA plasma layer deposited in PW mode at 20 W and 0.7 sccm monomer flow rate: a) C1s peak, b) N1s peak, and c) O1s peak.

Fitting of the C1s signal by three components, instead of four described above, was also tested but did not provide satisfactory agreement with the experimental data for reasonable values of the binding energies (i.e., deviation with the literature less than 0.2 eV) and the FWHM <2.0 eV for each the component. It can be seen from the C1s signal that the intensity at binding energy around 286.5 eV is high compared to the atomic concentrations of oxygen and nitrogen and, therefore, it is not possible to fit the measured data by taking into account only C═N and C—O bonds. Since the FT-IR spectra revealed the presence of nitrile and amine peaks, the high signal intensity at around 286.5 eV can be clearly explained by a consideration of **C**≡N and **C**—NH$_x$ environments of carbon. Additionally, the peak associated with the **C**—C≡N environment had to be considered due to a strong electron-withdrawing secondary effect of nitrile group.[27] However, according to the literature the BE of **C**—C≡N and **C**≡N groups are equal to 286.3 and 286.7 eV, respectively.[26] Such small difference in BE is insufficient to separate these two contributions in the spectra obtained by nonmonochromated XPS machine. Thus, these two contributions were attributed to one single peak at 286.5 eV.

The results of the C1s and N1s fitting are summarized in Table 4 and 5. It can be seen from Table 5 that the concentration of CH$_x$ groups is increasing whereas CN is decreasing with *W/F*. This confirms the results of FT-IR presented in Figure 4. It is important to observe changes of the NH$_x$ concentration independently of other functional groups. It can be most easily done by the fitting of N1s peak because the uncertainty of the fitting is higher in the case of C1s due to a larger number of the expected peaks with close BE. It appears from Figure 7 that the PW plasma polymers bear higher concentration of NH$_x$ groups (at%) than the CW plasma polymers at a similar *W/F*. The concentration of **N**H$_x$ for the PW layers fluctuates around 9 at% for low *W/F* and than decreases down to 6 at% (Table 4 and Figure 7). In the case of the CW films, the concentration of **N**—H$_x$ is around 5.7 at% and the significance of its dependence on *W/F* is questionable because of low number of samples. However, the existence of a maximum for the CW layer prepared at $W/F = 384$ eV was confirmed by the fitting of C1s and evolution of the **C**—NH$_x$ concentration with *W/F* (Table 5).

The concentration of **C**═O/N—**C**═O carbon environment (amide, ketone, and acetal groups) is always higher compared to **N**—C═O environment (amide group) calculated from N1s curve fitting and thus we should consider that two types of carbon environment ketone and acetal and amide groups are both presented in the plasma polymer. Furthermore, the O1s curve fitting (Figure 6c) has also confirmed that two types of oxygen environments: **O**—C—**O** and —C═**O** and **O**═C—N are incorporated in the plasma coating with the ratio **O**—C—**O** and —C═**O**/**O**═C—N being approximately 40:60. Hence, the CPA plasma polymers contain several types of "oxidized" carbon that are probably induced by reactions with oxygen or moisture from the atmosphere.

In conclusion, the combination of two characterization methods, FT-IR and XPS, provided comprehensive information about the chemical structure of CPA plasma polymers and the methods were supporting each other. The variation of the monomer flow rate, i.e., variation of the *W/F*, affected the CPA plasma layer chemistry. However, this parameter

Table 4. XPS N1s environments in at% of the CPA plasma polymers as deposited (before immersion in H_2O) and after immersion in H_2O.

Disch. mode, *W/F* [eV]	**N—H_x [at%]**		**N≡C [at%]**		**N—C=O [at%]**	
	Before	**After**	**Before**	**After**	**Before**	**After**
	Immersion in water		**Immersion in water**		**Immersion in water**	
PW, 88	8.5	5.6	9.5	6.4	1.8	3.6
PW, 127	9.2	4.7	8.3	7.1	1.3	3.9
PW, 296	8.6	4.9	7.7	5.7	0.9	3.3
PW, 887	7.0	4.3	6.4	6.2	2.9	3.3
CW, 268	4.7	1.6	10.5	8.2	1.0	1.2
CW, 384	6.7	4.8	6.7	5.3	1.2	3.0
CW, 896	5.7	2.4	3.3	2.8	2.0	1.8

The duration of the immersion is equal to 48 h for PW plasma layers while CW layers were immersed for 1 h.

Table 5. XPS C1s environments of the CPA plasma polymers as deposited (before immersion in H_2O) and after immersion in H_2O.

Disch. mode, *W/F* [eV]	**CH_x [at%]**		**C—NH_x [at%]**		**C—C≡N/C≡N [at%]**		**C=O and N—C=O [at%]**	
	Before	**After**	**Before**	**After**	**Before**	**After**	**Before**	**After**
	Immersion in water		**Immersion in water**		**Immersion in water**		**Immersion in water**	
PW 89	41.6	45.3	7.1	4.8	26.1	23.3	3.2	5.3
PW 127	40.0	41.1	8.6	6.2	23.8	22.8	4.5	6.6
PW 296	44.0	42.4	6.2	5.0	23.5	23.2	3.7	6.7
PW 887	50.8	49.9	5.6	5.6	17.1	17.1	4.5	6.3
CW 268	45.7	38.3	4.6	1.2	25.1	15.6	3.6	5.8
CW 384	43.1	50.1	5.4	3.9	25.9	19.6	5.6	5.6
CW 896	67.1	66.1	2.6	2.9	9.7	8.2	3.7	4.9

The duration of the immersion is equal to 48 h for PW plasma layers while CW layers were immersed for 1 h.

does not control it independently of the discharge mode, CW or PW, because the discharge pulsing is more efficient at keeping the monomer structure during plasma polymerization. Thus, the N/C ratio, **N**H_x and **C**—NH_x environments as well as the N—H stretching and NH_x scissoring intensities of PW plasma polymers are higher compared to the layers deposited in CW discharge at a similar *W/F*. It is interesting to notice that at low *W/F* the amines are sacrificed in favor of nitriles. However, at higher *W/F*, the concentration of nitriles is also decreasing, which leads to an overall decrease of the nitrogen concentration in the layers.

3.2. Optical Emission Spectroscopy of CPA Plasma

A question on the nature of nitrile groups formation arose in the previous section because the layers contained a relatively high amount of these groups at low *W/F* although the monomer does not have these groups in its original structure. The nitrile groups can be generated in the plasma volume and incorporated in the layers or they can be formed directly at the surface due to the reaction between surface radicals and the monomer. The OES of CPA discharges was performed under different plasma conditions in order to get more insight into the origin of nitrile groups and an overview of the plasma excited species.

All the emission spectra contained emission of CN (the violet system $B^2\Sigma^+ \rightarrow X^2\Sigma^+$ and the red system $A^2\Pi \rightarrow X^2\Sigma$), CH ($A^2\Delta \rightarrow X^2\Pi$, 431.3 nm), NH ($A^3\Sigma \rightarrow X^3\Sigma$, 336 nm), H_α (656.3 nm), and H_β (486.1 nm) that are typically present in the CH_4/N_2 and allylamine plasmas.[35,36] The CN emission dominated the spectra because three intense bands of the violet system appeared in the regions 358–359, 385–388, 415–422 nm, and the bands of the red system were

DOI: 10.1002/ppap.201300177

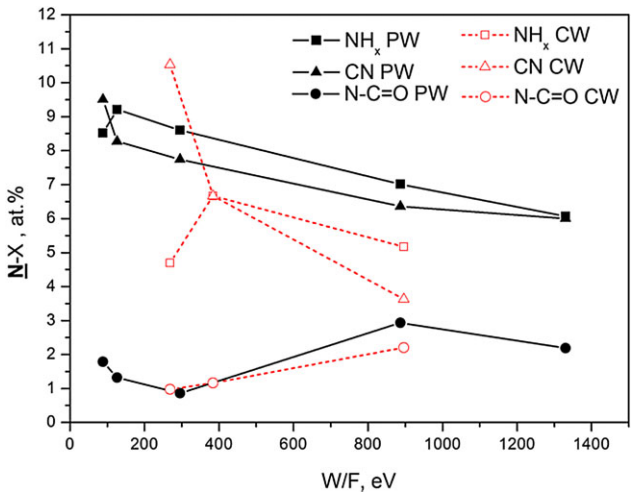

Figure 7. Evolution of XPS N1s components with the *W/F* for the films deposited in PW and CW discharges.

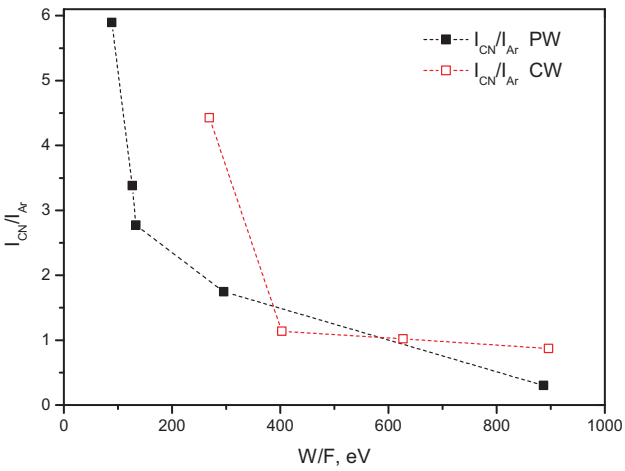

Figure 9. Ratio of the intensity of CN emission (388.3 nm) over Ar line (696.5 nm) as a function of *W/F*.

distributed above 500 nm.[37] Several Ar atomic lines were detected, the most intense at 696.5, 706.7, and 738.4 nm. Nitrogen impurity was indicated by a very weak band of the second positive system $C^3\Pi \rightarrow B^3\Pi$ detected at 315.9 and 375.5 nm. The very weak band of the OH system ($A^2\Sigma \rightarrow X^2\Pi$) detected at 306–330 nm indicated the presence of water impurity. A typical spectrum of the CPA glow discharge is given in Figure 8, here for CW plasma at 20 W and monomer flow rate of 0.3 sccm.

The CN, CH, and NH emission bands and H atomic lines provides information about the dissociation of the monomer although indirectly through the formation of excited species. The presence of CN emission shows that nitrile groups can be formed in the plasma phase. The intensity of CN band head at 388.3 nm divided by the intensity of Ar line at 696.5 nm was studied in dependence on the *W/F* (Figure 9). In first approximation, this ratio can be used to estimate changes in the concentration of CN radicals independently of changes in electron density assumed the electron energy distribution function is not changing with the variation of *W/F*. The ratio of the CN intensity over Ar (I_{CN}/I_{Ar}) is decreasing rapidly with *W/F*. It is interesting that the concentration of nitriles in the plasma is the highest at low *W/F*. The CN radicals are products of the monomer dissociation and further chemical processes in the plasma. The high energy input either does not favor degradation of CPA into CN or causes further decomposition of the intermediate CN product.

The comparison of Figure 7 and 9 shows how the behavior of CN emission correlates with the above reported dependence of the nitrile groups concentration on *W/F*. An unexpectedly high **N**≡C concentration was determined for the CW layer deposited at *W/F* = 269 eV (Figure 7 and Table 4). It can imply that the CN radicals formed in the plasma govern the incorporation of nitrile groups in the coating, i.e., the origin of the nitrile groups relies on the CPA plasma chemistry. However, a deeper investigation of the CPA plasma chemistry and understanding of the chemical pathway including all dissociation and recombination reactions leading to the formation of the CN radicals are out of scope of this work. This work aims to deposit amine-rich films that are stable in aqueous media and, therefore, the major part of the paper is focused on the characterization of the films deposited at different plasma conditions and the investigation of their interaction with water as given in the next section.

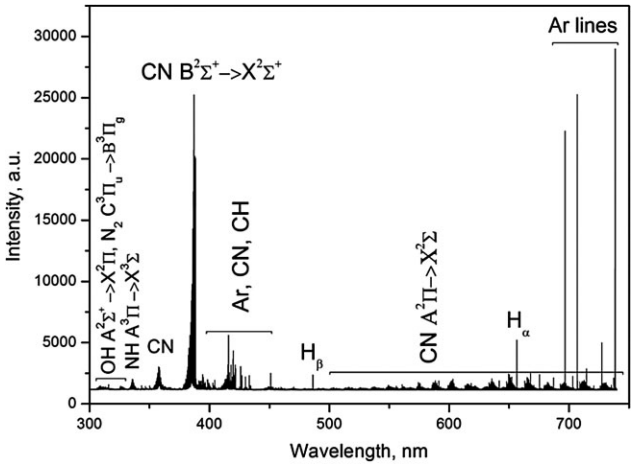

Figure 8. Typical OES spectrum obtained from the CPA plasma at 20 W, in CW mode and using monomer flow rate of 0.3 sccm.

3.3. Stability of Plasma Polymers in Water

3.3.1. Thickness Loss and Morphological Changes

According to the literature, one of the common methods aimed at the investigation of the layer stability in water is

the monitoring of the thickness loss during the immersion in deionized water.[6,13,14] It is considered that this stability is correlated with the number of the polar groups presented in the coating and the thickness loss is increasing with their concentration. Another important parameter affecting the stability of the plasma layer is the presence of oligomeric (low molecular weight) constituents in the polymer structure. These oligomers release rapidly upon a contact with water. Thus, the CPA plasma polymers were immersed into the deionized water for three different durations: 1, 24, and 48 h in order to distinguish the effect of the dissolution of the plasma layer due to affinity of polar groups toward the water and the possible influence of the oligomeric constituents.

The thickness residue was calculated as the film thickness after immersion in water divided by the original (as-deposited) thickness. This ratio is plotted in Figure 10 in dependence on *W/F*. A significantly different result was obtained for the CW film deposited at low *W/F* because this film was almost completely removed by water immersion. The SEM micrographs in Figure 11e showed debris of the film.

Other films were more stable in water and it can be seen from Figure 10 that the most significant thickness loss appeared within first hour of the layer immersion. Then the thickness of the CPA plasma polymers becomes quite stable and no significant change of the thickness was observed after 48 h of immersion compared to the layer immersed for 24 h. If the thickness loss was related to the interaction between polar groups of plasma polymer and H_2O molecules, then the thickness loss would be dependent on the concentration of nitrogen, as it was reported before for acetylene/ammonia plasma deposits.[13] Comparing

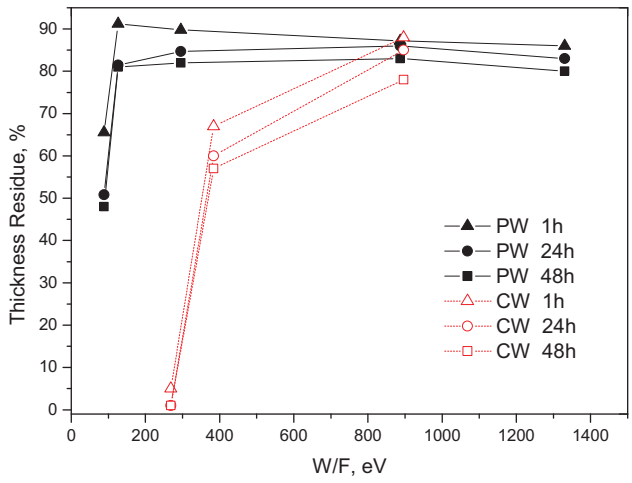

Figure 10. Thickness residue as a function of *W/F* for PW and CW films immersed in water for 1, 24, and 48 h. The initial film thickness was 280 ± 30 nm except the PW layers deposited at the *W/F* ≥ 887 eV that had thickness of 120 nm.

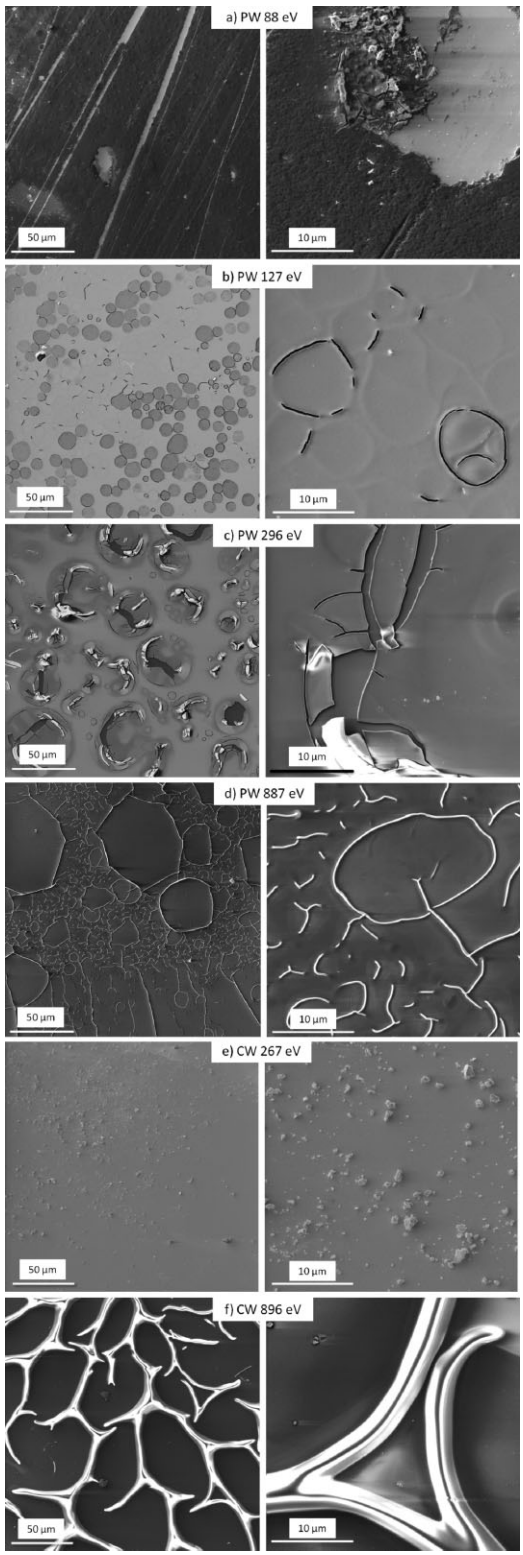

Figure 11. Low (left) and high (right) magnification SEM micrographs of the layers after 48 h immersion in water. The *W/F* and discharge mode are given in the figures, the on-time power was 20 W and the monomer flow rates were: a) 1.0 sccm, b) 0.7 sccm, c) 0.3 sccm, d) 0.1 sccm, e) 1.0 sccm, and f) 0.3 sccm.

Figure 5 and 10, it becomes evident that the evolution of N/C ratio and the thickness residue does not support this hypothesis. The N/C ratio is decreasing importantly with W/F whereas the thickness residue after 1 h immersion is almost constant for the plasma polymers synthesized at $W/F = 126–1\,330$ eV. On the other hand, the PW layers deposited at W/F of 88 and 126 eV have similar N/C but the thickness residue of the latter is higher by 35%. Hence, there is no direct correlation between the concentration of polar groups in CPA plasma polymers and their stability in water. Therefore, it is proposed that major reason for the thickness loss is related to the dissolution of the oligomers in contact with water and hydrolysis of the films. The chemical analyses of the surfaces after the immersion in water, reported in the next section, were performed to support this conclusion.

SEM imaging of the films after immersion in water helped to understand the differences in behavior of CPA plasma polymers in contact with water. The as-deposited films were so smooth that no visible features were observed by SEM. Their immersion into water induced significant changes in the surface morphology as shown in Figure 11. The appearance of the damage and its extent depended on the conditions of plasma polymerization.

The coating deposited in PW plasma using 1 sccm of CPA (and lowest W/F) was swallowed and partially delaminated (Figure 11a). The layer could delaminate because of the stress induced during the deposition followed by the loss of adhesion due to water immersion or because of the stress induced by the interaction with water. Since XPS did not detect signal of silicon the latter explanation is more probable because the delamination did not occur at the interface between the film and the substrate.

By decreasing the monomer flow rate and, i.e., increasing W/F, the type of damage in the PW coating was changed substantially. The delamination of the coating was not observed for the flow rate of 0.7 sccm, i.e., $W/F = 127$ eV, but SEM micrographs (Figure 11b) revealed round-shape defects with the radius of 10–15 μm. At even lower CPA flow rates, the size of round-shape defects increased. The SEM micrograph in Figure 11c obviously shows large area cracks. However, the XPS analyses (Table 3) did not support the conclusion that these cracks are interfacial cracks causing a film delamination because no silicon signal was detected.

A quite different appearance of film defects was observed for the CW plasma polymer prepared at high W/F (Figure 11f). The SEM micrographs show very similar defects to those observed in compressively stressed hydrogenated carbon films.[38,39] However, again, XPS did not revealed the Si2p signal and therefore no delamination at the substrate-coating interface was observed. Thus, the cracking occurs inside the film due to the stress release. Nevertheless, the stress of the as-deposited coating (in this condition) is equal to 25 ± 5 MPa, i.e., is relatively low. Therefore, it seems that the stress is drastically increased by the interaction with water. Vasilev et al.[14] considered that the stresses after immersion into the water are induced by the dissolution of oligomeric constituents causing shrinkage of the film and as a result formation of cracks in the surface. According to the published results, the density and size of the pores decreased with the applied power, while in the present case the behavior is more complex, as, e.g., the layer deposited with W/F of 896 eV exhibits a stronger damage compared to the layer deposited at W/F of 127 eV, where a higher fraction of the oligomers can be expected. Therefore, the origin of the stress cannot be caused only by the formation of the voids induced by the dissolution of low molecular weight fragments from the plasma polymer. It seems that water molecules penetrate into the bulk of the film and induce chemical gradients in the coating, causing the stress and, as a result, buckling of the coating. The confirmation of this hypothesis is out of the objectives of this paper.

3.3.2. Chemical Changes Induced by Immersion in Water

As expected from the thickness loss, the FT-IR spectra of the CW film deposited at 268 eV dramatically changed after 1 h immersion in water. The intensity of the peaks decreased almost to the level of noise due to the very low film thickness (below 5 nm) but the peaks belonging to CH_x stretching and amide II band were still detectable. XPS also did not indicate a complete delamination/dissolution of the film because the surface composition could not be explained as a native silicon oxide with some hydrocarbon contamination (Table 3).

The CPA plasma polymers, excluding the CW layer deposited at $W/F = 268$ eV, exhibited common chemical changes induced by the immersion in water and these changes are discussed below. A representative example of FT-IR spectra after 1, 24, and 48 h immersion in water is shown in Figure 12 for the PW layer deposited at $W/F = 127$ eV. The intensities of the double peak at about 2 200 cm^{-1} (C≡N, C≡N—, —N═C═N—), NH_x stretching, and NH_2 scissoring peaks decreased after the immersion in water although the absorbance was normalized to the thickness of layers. Additionally, the peak at ≈1 650 cm^{-1} became very broad or even split into two peaks for the PW film deposited at $W/F = 887$ eV. It could be caused by an addition of the amide bands: C═O stretching and NH bending. Thus, FT-IR shows that the immersion in water leads not only to the thickness loss but also to the chemical re-arrangement in the films. It is worth noting that no particular differences in the spectra were observed when comparing 24 and 48 h of immersion and, therefore, the layers did not suffer further detectable degradation after the 24 h of immersion.

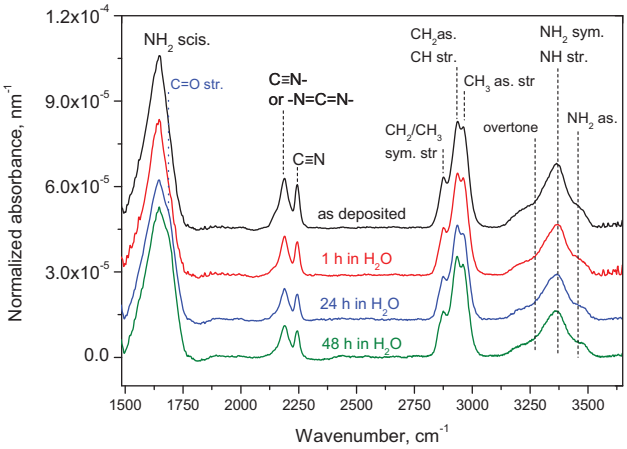

Figure 12. Normalized absorbance of CPA plasma polymers deposited in PW plasma at 20 W and 0.7 sccm: as deposited and after 1, 24, and 48 h of immersion in water.

According to XPS results in Table 3, the concentration of carbon does not changed after immersion in water, as the variation of 1 at% corresponds to the accuracy of the measurements. On the other hand, the concentration of nitrogen was decreased by 3–4 at% for all layers while the concentration of oxygen was increased by the same 3–4 at%. Therefore, the substitution of nitrogen by oxygen occurred during the immersion in the water, e.g., through the hydrolysis of imines C═NH.

In order to analyze the changes in the functional composition of the plasma polymers after immersion in water, the N1s and C1s environments are reported in Table 4 and 5. From Table 4, it can be seen that **N**≡C and/or **N**H_x environments decreased by 2–4 at%. At the same time, the CPA plasma polymers deposited with *W/F* up to 384 eV gained the concentration of amide environment **N**—C═O by ≈2 at%. Therefore, a well-known partial oxidation of the amine groups occurred. Nevertheless, the concentrations of **N**H_x and **N**≡C environments decreased more significantly compared to the increase of the amide groups concentration. The additional processes leading to the loss of nitrogen during immersion will be discussed in the next section.

Concerning the C1s environments (Table 5), it appears that the **C**—NH_x, **C**—C≡N/**C**≡N, and **C**═O/N—**C**═O were affected importantly by the contact with water. First of all, both **C**—NH_x and **C**—C≡N/**C**≡N environments were decreasing while the **C**═O/N—**C**═O component was significantly increased after immersion. Nevertheless, the concentration of **C**═O/N—**C**═O carbon environment is always lower compared to the atomic concentration of oxygen and the difference of 2–3 at% cannot be simply related to the accuracy of the XPS experiment. Therefore, around 2 at% of the oxidized carbon environment (most probably C—O) were not explained by the presented model of the C1s curve fitting. A separate **C**—O peak was not implemented into the C1s curve fitting because it would significantly complicate the fitting procedure. Therefore, it should be kept in mind that after the immersion the **C**≡N environment is also covering a small part (2–3 at%) of the **C**—O environment. In order to explain the possible phenomena induced by immersion in water, the possible chemical reactions between CPA plasma polymer and water molecules are discussed below.

4. Conclusion

The CPA plasma polymers were prepared in capacitively coupled RF discharges in continuous and pulsed (DC of 33%) wave modes. The FT-IR and XPS analyses revealed complex structure of these plasma polymers containing hydrocarbon chains, primary and secondary amines, nitriles, and possibly imines. The *W/F* influenced their chemical structure but it did not control it independently of the discharge mode. A higher retention of the monomer structure was obtained for pulsed discharges even though *W/F* was similar. Using pulsed discharges, the films with N/C ratio above 0.24 (the perfect CPA polymer should bear N/C = 0.33) were deposited at higher monomer flow rates 0.7–1.0 sccm. These films contained relatively high amount of amine groups (**N**H_x up to 9.2 at%) as evidenced by the fitting of XPS N1s signal. At the optimized monomer flow rate of 0.7 sccm, the PW film exhibited only 20% thickness loss after 48 h immersion in water. The oxygen concentration introduced by immersion in water was 4 at% and the film still contained about 5 at% of the **N**H_x environment at the surface. The degradation of PW CPA plasma polymers is lower compared to reported stability test of allylamine plasma polymers and comparable with the results of the most stable amine plasma deposits, namely C_2H_4:NH_3 (ratio ≈2:1) plasma layers.[6,9,11]

Acknowledgements: This work was supported by the project "Employment of Newly Graduated Doctors of Science for Scientific Excellence" (Grant No. CZ.1.07/2.3.00/30.0009) co-financed by the European Social Fund and the State Budget of the Czech Republic. This work was realized in CEITEC – Central European Institute of Technology with research infrastructure supported by the project CZ.1.05/1.1.00/02.0068 financed from European Regional Development Fund.

Received: November 15, 2013; Revised: February 14, 2014; Accepted: February 17, 2014; DOI: 10.1002/ppap.201300177

Keywords: amine coatings; cyclopropylamine; ESCA/XPS; FT-IR; pulsed discharges

[1] K. Siow, L. Britcher, S. Kumar, H. Grieser, *Plasma Process. Polym.* **2006**, *3*, 392.
[2] M. Muller, C. Oehr, *Surf. Coat. Technol.* **1999**, *802*, 116.

[3] H. Biederman, I. Boyaci, P. Bilkova, D. Slavinska, S. Mutlu, J. Zemek, M. Trchova, J. Klimovic, M. Mutlu, *J. Appl. Polym. Sci.* **2001**, *81*, 1341.
[4] J. Borris, M. Thomas, C. Klages, F. Faupel, V. Zaporojtchenko, *Plasma Process. Polym.* **2007**, *6*, S258.
[5] R. Nakamura, H. Muguruma, K. Ikebukuro, S. Sasaki, R. Nagata, I. Karube, H. Pedersen, *Anal. Chem.* **1997**, *69*, 4649.
[6] J. Ruiz, A. St-Georges-Robillard, C. Thérésy, S. Lerouge, M. Wertheimer, *Plasma Process. Polym.* **2010**, *7*, 737.
[7] R. C. Chatelier, X. Xie, T. R. Gengenbach, H. J. Griesser, *Langmuir* **1995**, *11*, 2576.
[8] ScienceLab: Chemicals and Laboratory Equipment, MSDS of allylamine, http://www.sciencelab.com/msds.php?msdsId=9922832, accessed: November 2013.
[9] B. Finke, K. Schroder, A. Ohl, *Plasma Process. Polym.* **2009**, *6*, S70.
[10] K. Jarvis, P. Majewski, *ACS Appl. Mater. Interfaces* **2013**, *5*, 7315.
[11] A. Abbas, C. Vivien, B. Bocquet, D. Guillochon, P. Supiot, *Plasma Process. Polym.* **2009**, *6*, 593.
[12] Z. Zhang, Q. Chen, W. Knoll, R. Foerch, R. Holcomb, D. Roitman, *Macromolecules* **2003**, *36*, 768.
[13] A. Contreras-Garcia, M. R. Wertheimer, *Plasma Chem. Plasma Process.* **2013**, *33*, 147.
[14] K. Vasilev, L. Britcher, A. Casanal, H. Griesser, *J. Phys. Chem. B* **2008**, *112*, 10915.
[15] L. Denis, P. Marsal, Y. Olivier, T. Godfroid, R. Lazzaroni, M. Hecq, J. Cornil, R. Snyders, *Plasma Process. Polym.* **2010**, *7*, 172.
[16] P. Girard-Lauriault, P. Dietrich, T. Gross, T. Wirth, W. Unger, *Plasma Process. Polym.* **2013**, *10*, 388.
[17] S. Voronin, M. Zelzer, C. Fotea, M. Alexander, J. Bradley, *J. Phys. Chem. B* **2007**, *111*, 3419.
[18] D. Hegemann, E. Korner, S. Guimond, *Plasma Process. Polym.* **2009**, *6*, 246.
[19] D. Hegemann, U. Shultz, E. Korner, *Plasma Process. Polym.* **2011**, *8*, 689.
[20] A. Manakhov, M. Moreno-Couranjou, P. Choquet, N. Boscher, J.-J. Pireaux, *Surf. Coat. Technol.* **2011**, *205*, 466.
[21] A. Manakhov, M. Moreno-Couranjou, P. Choquet, N. Boscher, J.-J. Pireaux, *Plasma Process. Polym.* **2012**, *9*, 435.
[22] L. Zajíčková, V. Buršíková, D. Franta, A. Bousquet, A. Granier, A. Goullet, J. Buršík, *Plasma Process. Polym.* **2007**, *4*, S287.
[23] F. Chen, J. Chang, *Principles of Plasma Processing*, Plenum/Kluwer Publichers, Los Angeles, CA, USA **2002**.
[24] D. Hegemann, M. Hossain, *Plasma Process. Polym.* **2005**, *2*, 554.
[25] M. Mohai, *Surf. Interface Anal.* **2004**, *36*, 828.
[26] G. Beamson, D. Briggs, *High Resolution XPS of Organic Polymers*, Wiley &Sons, Chichester, England **1992**.
[27] A. Karim Oultache, R. E. Prud'homme, *Polym. Adv. Technol.* **2000**, *11*, 316.
[28] D. Franta, D. Nečas, L. Zajíčková, *Opt. Express* **2007**, *15*, 16230.
[29] D. Nečas, I. Ohlídal, D. Franta, *J. Opt.* **2011**, *13*, 085705.
[30] L. Zajíčková, D. Franta, D. Nečas, V. Buršíková, M. Muresan, V. Peřina, C. Cobet, *Thin Solid Films* **2011**, *519*, 4299.
[31] Y. Zhang, S. Lau, D. Sheeja, B. Tay, *Surf. Coat. Technol.* **2005**, *195*, 338.
[32] G. Socrates, *Infrared and Raman Characteristic Group Frequencies. Tables and Charts*, Wiley & Sons, Chimester, England **2004**.
[33] D. W. Mayo, F. Miller, R. Hannah, *Interpretation of Infrared and Raman Spectra*, Wiley &Sons, New Jersey, USA **2004**.
[34] T. R. Gengenbach, Z. R. Vasic, R. C. Chatelier, H. J. Griesser, *J. Polym. Sci. A: Polym. Chem.* **1994**, *32*, 1399.
[35] K. J. Clay, S. P. Speakman, G. A. J. Amaratunga, S. R. P. Silva, *J. Appl. Phys.* **1996**, *9*, 79.
[36] D. Thi Tran, S. Mori, D. Tsuboi, M. Suzuki, *Plasma Process. Polym.* **2009**, *6*, 110.
[37] R. W. B. Pearse, A. G. Gaydon, *The Identification of Molecular Spectra*, Vol. *297*, Chapman and Hall, London **1976**.
[38] L. Zajíčková, S. Rudakowski, H. Becker, D. Meyer, M. Valtr, K. Wiesemann, *Thin Solid Films* **2003**, *425*, 72.
[39] V. Buršíková, P. Dvořák, L. Zajíčková, D. Franta, J. Janča, J. Buršík, J. Sobota, P. Klapetek, O. Bláhová, V. Peřina, *Optoelectron. Adv. Mater. – Rapid Commun.* **2007**, *1*, 491.